Article DOI: https://doi.org/10.37284/eaje.7.1.2135

East African Journal of Engineering
eaje.eanso.org
Volume 7, Issue 1, 2024
Print ISSN: 2707-5389 | Online ISSN: 2707-5397
Title DOI: https://doi.org/10.37284/2707-5397

EAST AFRICAN NATURE & SCIENCE ORGANIZATION

Original Article

Smoothing of the Noisy Lithium-ion Battery Surface Temperature Data Based on Savitzky–Golay (SG) Filter

Jordan H. Hossea[1*] *& Kenedy Greyson*[1]

[1] Dar es Salaam Institute of Technology, P. O. Box 2958 Dar-es-salaam, Tanzania.
* Author for Correspondence Email: jordan.hossea@dit.ac.tz

Article DOI : https://doi.org/10.37284/eaje.7.1.2135

Publication Date:

25 August 2024

Keywords:

Battery Thermal Management System, Lithium-Ion Batteries, Noisy Data, Savitzky-Golay Filter, SNR

ABSTRACT

As the charging current and surrounding temperatures rise concurrently in an electric vehicle's (EV) battery pack, the battery temperature increases abruptly beyond safe limits. The battery is susceptible to triggering thermal runaway at higher temperatures, leading to battery damage and even an explosion. The control system depends on these measurement data from the sensors to prevent dangerous situations and maximize the performance and cycle life of batteries. However, traditional noisy temperature measurement sensors in a real application, such as thermistors and thermocouples, are extensively used. In this paper, the experimental setup, the heat pipe-based battery thermal management system (BTMS) was designed and experimented with high input power. The battery was sandwiched with heat pipes, and heated at 30, 40, 50, and 60 W. The Savitzky-Golay filter technique is applied to the noisy temperature data of the surface temperature of the lithium-ion batteries (LIBs) used to estimate the condition of the battery. According to this study, the start-up time parameter in battery thermal management can be controlled by the Savitzky-Golay filter. This will attenuate random temperature fluctuations of battery temperature noise and avoid the cooling system from being falsely triggered. The results are measured by the signal-to-noise (SNR) to demonstrate the ability of the Savitzky-Golay filter to eliminate noise.

APA CITATION

Hossea, J. H. & Greyson, K. (2024). Smoothing of the Noisy Lithium-ion Battery Surface Temperature Data Based on Savitzky–Golay (SG) Filter *East African Journal of Engineering*, 7(1), 262-271. https://doi.org/10.37284/eaje.7.1.2135

CHICAGO CITATION

Hossea, Jordan H. and Kenedy Greyson. 2024. "Smoothing of the Noisy Lithium-ion Battery Surface Temperature Data Based on Savitzky–Golay (SG) Filter". *East African Journal of Engineering* 7 (1), 262-271. https://doi.org/10.37284/eaje.7.1.2135.

HARVARD CITATION

Hossea, J. H. & Greyson, K. (2024) "Smoothing of the Noisy Lithium-ion Battery Surface Temperature Data Based on Savitzky–Golay (SG) Filter", *East African Journal of Engineering*, 7(1), pp. 262-271. doi: 10.37284/eaje.7.1.2135.

IEEE CITATION

J. H., Hossea & K., Greyson "Smoothing of the Noisy Lithium-ion Battery Surface Temperature Data Based on Savitzky–Golay (SG) Filter" *EAJE*, vol. 7, no. 1, pp 262-271, Aug. 2024.

MLA CITATION

Hossea, Jordan H. & Kenedy Greyson "Smoothing of the Noisy Lithium-ion Battery Surface Temperature Data Based on Savitzky–Golay (SG) Filter" *East African Journal of Engineering*, Vol. 7, no. 1, Aug. 2024, pp. 262-271, doi:10.37284/eaje.7.1.2135.

Article DOI: https://doi.org/10.37284/eaje.7.1.2135

INTRODUCTION

There are different types of batteries nowadays. However, most electric vehicles (EVs) and various storage systems use Lithium-ion batteries (LIBs) [1-4]. Many of the attractive features of LIBs include high current, power, energy density, prolonged life cycle, no memory effect, and low self-discharge rate [5-8]. However, LIBs remain prone to thermal runaway, fire, and high temperatures [9]. The battery capacity is estimated based on the battery surface temperature change [10] and the performance of LIBs depends on the working temperature. Most of the temperature effects are related to chemical reactions occurring in the batteries and also to the materials used in the batteries [11]. The temperature generated during the time of discharging and charging, and the environmental temperature cause the destruction of the battery [12]. Therefore, to maximize the battery service life, the battery temperature must be monitored [13, 14]. The estimation of the state of health (SoH) of a Li-ion is of great significance to system safety and economic development [15, 16].

A battery thermal management system (BTMS) is an electronic device for controlling rechargeable batteries (battery packs or cells). It is a data-driven system, and one of the most important components of a battery management system (BMS) that ensures the cell capacity and longevity, system safety, and efficiency of battery performance. Therefore, temperature measurements are vital measurements during the estimation of the suitable operation, thermal safety in application, and condition of the battery. For a proper selection of the temperature measurement method, aspects such as measurement range, accuracy, resolution, and costs of the method are important. Other non-invasive measurements are the battery terminal voltage, the current, humidity, and the physical expansion of battery cells. Among all, temperature significantly affects capacity, voltage, internal resistance, discharge/charge state, lifetime, safety, and inhomogeneity [17]. Although the chemical reaction is faster when the temperature rises in the battery, the thermal runaway occurs, the chemicals get lost and this decreases the life of a battery. Similarly, when the temperature is low the chemical may freeze. Because of that, BTMS requires temperature-changing data accuracy at the rate of 1/s (1 Hz).

The BTMS systems are utilized to improve the battery efficiency, by keeping the battery temperature within desired ranges and guaranteeing the allowable temperature limits for the battery pack. To protect batteries from potential damage, the excess temperature must be closely monitored to avoid any possibility of leakage or any cause of fire. Hence, the battery management depends on the estimation of the internal temperature. Both high and low temperatures have important effects on the SoH of LIBs [15, 16]. Due to the heterogeneous internal resistances of cells, heat generations are different and there are thermal gradients within the battery pack. In general, cell degradation is faster at higher temperatures [10]. The operating temperature of various types of batteries is shown in Table 1. The reliable and safe performance of the working temperature should be in the range of 15-35◦C [11, 18]. Under typical conditions, the temperature differences between the battery surface and core can be 10 K or more [19]. The internal or the core temperature is always beyond the surface temperature such that before the surface temperature reaches the temperature limit, the core temperature is already beyond the limit.

Table 1: Temperature ranges for different power batteries [17, 20].

Battery type	Operating temperature (ºC)	Cycle life
Nickel Cadmium (Ni–Cd)	−20~50 °C	>800
Nickel-Metal Hydride (Ni–MH)	−20~60 °C	>800
Lead Acid	−10~50 °C	>300
Lithium Ion (Li-ion)	−20~60 °C	>1000

Article DOI: https://doi.org/10.37284/eaje.7.1.2135

Core temperature simultaneous estimation is necessary for BMS to diagnose thermal runaway reactions and protect batteries from potential damage. The charger reduces the voltage supply to ensure peak charging when the battery temperature is high to avoid overheating. Similarly, during low temperatures, the charger uses a higher voltage to the battery to offset the increased resistance caused by the low temperature [10, 21]. The BTMS consists of temperature sensors across the surface of a battery pack, cooling systems, and heating systems in heat transport from or to the battery cells. Cooling systems use air; either forced where fans are used to induce airflow or natural air cooling where natural air cooling is used [22]. Air thermal management is less expensive and requires minimum space [23]. Unless a well-designed and arranged channel and cooling system has low thermal conductivity of air. However, air as a thermal management medium suffers from low heat capacity when it comes to managing large battery packs. Liquids, on the other hand, possess much higher heat capacity than air [24]. Direct liquid cooling is where batteries are kept in direct contact with the liquid coolant and indirect cooling is where the coolant flows in tubes, cold plates, or jackets that are in contact with the surface of the batteries. Applications of direct cooling strategy are used in high-performance vehicles where indirect cooling systems are used where safety and state of health requirements are high such as in passenger electric vehicles. Although the liquid cooling systems require a more complex design, they ensure the cells operate within the temperature limits. On the other hand, phase change materials (PCMs) can regulate heat since they undergo a phase change and absorb heat energy as a result. During the temperature drops, the phase change reverses and the PCM releases heat. This approach is used for thermal management in buildings, and electric vehicles (EVs). However, PCMs have low thermal conductivity but can be improved by mixing nanoparticles with pure PCM. Pure PCM-based system performance can be further improved by using it with some active cooling techniques such as forced air cooling for cylindrical batteries.

Generally, the temperature and/or voltage measurements contain noises in a real application, and these interferences will be further amplified by the differential operation if the adopted voltage interval is too small. Most of the presented work use different types of filter namely; the Savitzky-Golay filter [25, 26], dual filtering [25, 26], least square moving window [27], Kalman filter [28] and recursive least squares (RLS) [6] to improve signal to noise ratio in the in the voltage contain noise and minimizing error in on state of charge estimation. Thus, to prevent the cooling system from activating incorrectly, no study has shown how to use a Savitzky-Golay filter to smooth the battery's maximum temperature and surface temperature. Note that the startup time is the crucial factor influencing battery thermal management performance. The "Start Time" parameter indicates that a delay should be applied before the battery is cooled up [29]. If the start-up time is not taken into account, the lithium-ion battery will overcool, which will cause the diffusion process of the Li-ion battery to slow down and its chemical reaction to deaccelerate [29]. The sensor needs to be mounted on the battery surface in order to automate this kind of procedure. The cooling system is turned on by the controller after receiving a signal from the sensor. But when the electric car is moving, the noise will have a significant impact on it. This will lead to erratic variations in the temperature difference and surface temperature, which will cause the cooling system to be falsely triggered or activated.

METHODOLOGY

Theoretical formulation

Nevertheless, no study has tackled this problem and suggested the Savitzky-Golay filter to reduce the impact of noise without altering the original signal, according to the review conducted by researchers. Furthermore, the Savitzky-Golay filter can keep the waveform's peak and shape. The noise from the Savitzky-Golay filtering of the LIB surface temperature is filtered in this article by adjusting the Savitzky-Golay filter.The

Article DOI: https://doi.org/10.37284/eaje.7.1.2135

Savitzky-Golay filters are a type of Finite Impulse Response (FIR) digital filter derived directly from a particular formulation of the data smoothing problem in the time domain [30, 31]. The filtering process forms the least squares polynomials fitting the data where the number of sampling points considered in a group is defined by the window size parameter while controlling the order of the used polynomial [32, 33]. The mathematical description of the smoothing process implemented by Savitzky-Golay filtering is expressed by (1) [34-37].

$$s_j^* = \sum_{x=-m}^{m} \frac{c_x s_{j+x}}{N} \tag{1}$$

where s is the original signal, s^* is the smoothed signal, c_x is the coefficient for the x^{th} smoothing, N is the number of data points in the smoothing window, and is equal to $2m+1$, and m is the half-width of the smoothing window. The index j represents the running index of the ordinate data in the original data table.

The essence of Savitzky-Golay filtering is adopting a polynomial in a sliding window to fit the original signal piece-by-piece depending on the least-squares estimation algorithm. The polynomial can be modelled as shown in (2) [33]. Given a set of $2m+1$ data values, the polynomial of n degree that satisfies the least squares fit of these values is expressed as [37].

$$f(x) = b_0 + b_1 x + b_2 x^2 + \_\_\_\_\_ + b_k x^k \tag{2}$$

where b_n is the coefficient of the polynomial, k is the polynomial degree.

The coefficient of the polynomial, b_n is obtained by applying the least-squares criterion expressed by (3).

$$\frac{\partial}{\partial b_n}\left\{\sum_{x=-m}^{m}\left[f_k(x) - s_x\right]^2\right\} = 0 \tag{3}$$

The b_0 is obtained by evaluating the (2) at $x = 0$, then b_n are obtained by computing the n^{th} differential of (2) at $x = 0$. Hence,

$$f_k^n(0) = \sum_{x=-m}^{m} c_x^n s_x \tag{4}$$

where n is the derivative order, c_x^n is the convolution weight, and s_x is the value of the x^{th} point.

The signal-to-ratio (SNR) is the qualitative measure of the level the noise present in the signal. SNR can be computed statistically as an expression shown in (5).

$$SNR = \frac{\sqrt{\left(\frac{1}{m}\sum_{i=1}^{m}\left(f(x_i) - \overline{f(x_i)}\right)^2\right)}}{\frac{1}{m}\sum_{i=1}^{m} f(x_i)} \tag{5}$$

Experimental setup and procedures

The setup diagram of the experiment is shown in Fig. 1. The composition includes an AC power supply, water pump, flow meter, re-circulating bath, and data logger. Using polyimide film (tape) the thermocouple is affixed. Data from the thermocouple on the LIBs are collected by the microcontroller-based data logger and communicated to the PC through the interface.

Experimental setup

The heating and cooling control is used to maintain the temperature at 30 °C. Heat generation inside the battery was set to 30, 40, 50, and 60 W and was controlled by an AC power supply. In this study, the heat generation rate (Qin) inside the aluminium plate depended on the input power of the heater, which could be controlled within the desired range. T-type thermocouples were used to measure the battery surface temperatures and the temperature of the inlet and outlet water. A data logger was used to collect temperatures from the battery surface at a sampling rate of 1 Hz.

Article DOI: https://doi.org/10.37284/eaje.7.1.2135

Fig. 1: Schematic diagram of the experimental setup

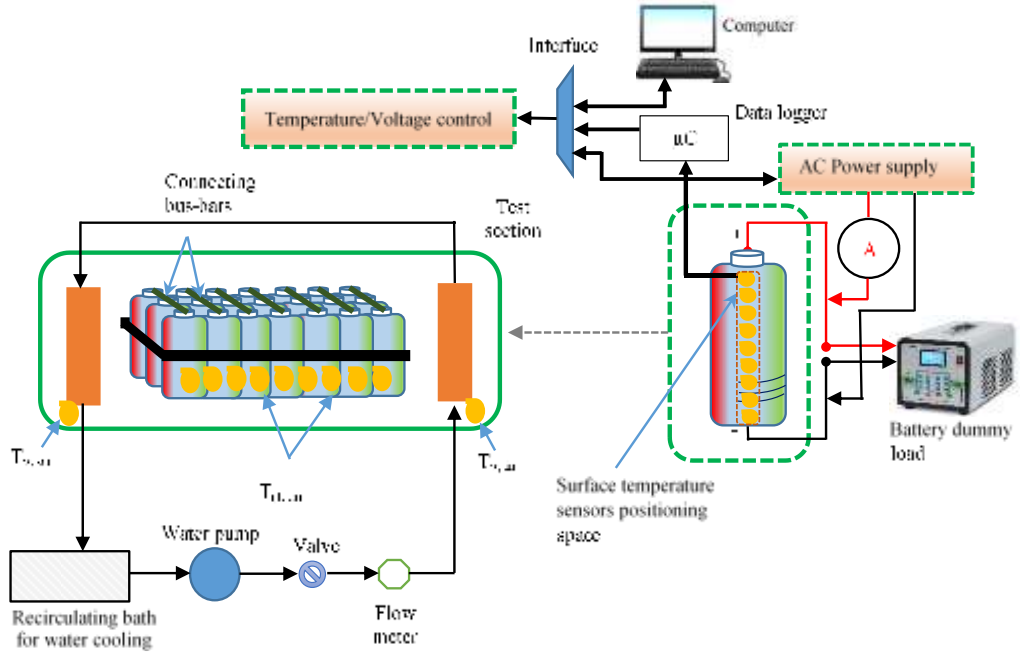

Experimental procedures

Initially, the temperature was maintained at 30 ◦C and then a heater was initiated at the power of 30 W. The temperature on the surface of the battery and the temperature of the inlet and outlet water were recorded. The heater was changed to 40 W, 50 W, and 60 W after every 2 hours while recording the surface temperatures. The heat generation rate (Q_{in}) inside the aluminium plate is expressed as shown in (6) [5].

$$Q_{in} = V \times I \tag{6}$$

where V is the voltage applied to the heater (V) and I is the current supplied to the heater rod (A).

Heat dissipation

Heat dissipated as heat radiation and heat convection (transferred to water), (Q_w) can be expressed as shown in Eqn. (7) [1, 5].

$$Q_W = m_w c_p (T_{w,out} - T_{w,in}) \tag{7}$$

where m_w is the water mass flow rate (kg/s), c_p is the specific heat of water (J/kg K), $T_{w,\,out}$ is the outlet water temperature (◦C), and $T_{w,\,in}$ is the inlet water temperature (◦C).

The mass flow rate is expressed as shown in Eqn. (8)

$$m_w = \rho q \tag{8}$$

where q is the water flow rate (m^3/s), and ρ is the density of water (kg/m^3).

RESULTS AND DISCUSSION

In this research work, the experiment shows that input power and water flow rate affect the maximum temperature (T_{max}), the minimum temperature (T_{min}), and the temperature difference (ΔT). The data were measured over one hour per each input power which were varied in the sequence of 30 W, 40 W, 50 W, and 60 W. The results in Fig. 2(a) and (b) show that as input power increases, the maximum battery surface temperature increases. The raw data has a maximum temperature of about 60 ˚C, meanwhile, the temperature difference rises to 7 ˚C. Again, the reported findings in Fig. 2(a) and (b) reveal that the raw data are impacted by noise, as evidenced by the random variation of the maximum temperature. Fig. 2 also demonstrates that without a Savitzky-Golay filter, the maximum temperature on the battery surface rises to roughly 61.20˚C, with a maximum temperature

Article DOI: https://doi.org/10.37284/eaje.7.1.2135

difference of 7 ˚C. The filter limits the maximum temperature difference to around 6˚C and the maximum battery temperature to 60.00 ˚C. The results show that without the Savitzky-Golay filter, the recorded maximum temperature and temperature difference result in an incorrect average temperature of ±1˚C. Deviations of ±1˚C are unacceptable for lithium-ion battery BMTS since they can cause false alarm triggering and BTMS actuation before the start-up time. It should be noted that the BTMS system should not be activated to cool the battery immediately after start-up since the heat has not yet accumulated. In the IOT-based BTMS monitoring system, a low signal-to-noise ratio increases the number of false alerts.

Furthermore, the results show that, when raw data was filtered for the first time using the Savitzky-Golay filter (1st SGF), fluctuation noise was decreased by 64.40 % in comparison to raw data. Furthermore, when the initial filtered data was put to the Savitzky-Golay filter for the second time (2nd SGF), the fluctuation noise was significantly decreased by 79.10 %, see Fig. 2(a). Similarly, when the temperature difference resulting from raw data was filtered for the first time using the Savitzky-Golay filter (1st SGF), fluctuation noise was reduced by 83.00 % in comparison to raw data. When the original filtered data was sent through the Savitzky-Golay filter for the second time (2nd SGF), the fluctuation noise decreased by 85.86 %, as shown in Fig. 2(b).

Fig. 2: (a) maximum temperature, T_{max} and (b) temperature difference, ΔT distribution on lithium-ion battery with application Savitzky–Golay filter is applied

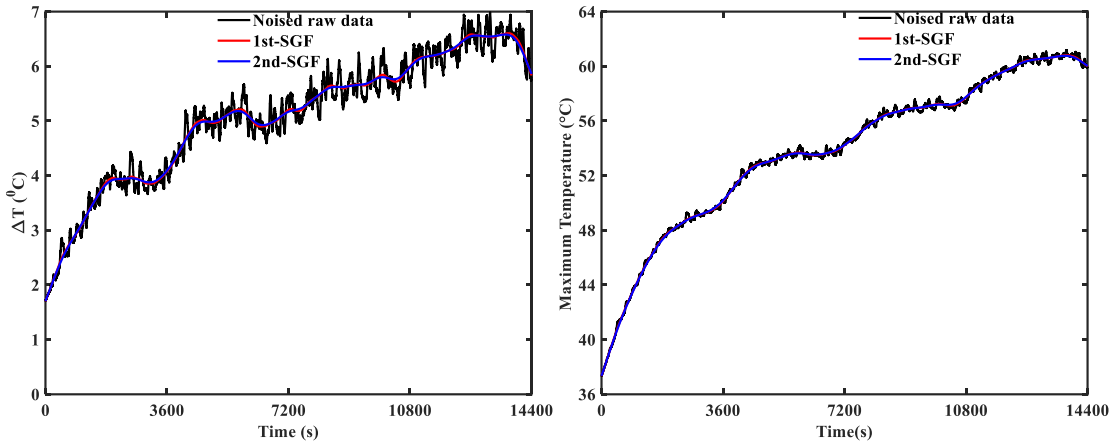

(a) (b)

MATLAB software is used to calculate the SNR using equation (5). The results in Table 2, demonstrated the Savitzky-Golay filter's ability to eliminate noise. Table 2 quantifies the signal-to-noise ratio of the raw data after it has been first and second filtered. The noise level on the maximum temperature lithium-ion battery and temperature differential are compared in the quantified result that is displayed. The findings reveal that the SNR of ΔT is lower than the maximum temperature of the battery, with a similar result presented in Fig. 2(a) and (b). As shown in Table 2, when the Savitzky-Golay filter is applied to the raw data, the SNR is increased from 6.4384 to 11.6485 dB, which is equivalent to 64.40% improvement of the signal, while the temperature difference shows an improvement of 83.00%, implying that the Savitzky-Golay filter can filter better for the signal with very low signal to noise ratio. The results demonstrate that when the first filtered signal (1st SGF) is filtered a second time using the Savitzky-Golay filter, the maximum surface temperature improves by 79.10%, while the temperature difference improves by 85.86 %. Thus, increasing the number of filters improves the signal-to-noise ratio.

Article DOI: https://doi.org/10.37284/eaje.7.1.2135

Table 2: SNR of the signal before and after application of the Savitzky-Golay filter

Signal	Max. temp. (SNR dB)	Temp. difference (SNR dB)
Raw data	6.4384	0.7222
1st SGF	11.6485	3.5279
2nd SGF	24.432	4.3857

Fig. 3 shows the effect of applying the Savitzky-Golay filter in multiple in the filtered signal. As seen, the filter is applied multiple times the signal-to-noise ratio of the signal increases. For the maximum temperature Figure 3(a) the SNR increases from 6.4384 to 123.8 dB, the trend is similar to the difference temperature in which SNR increases from 0.7722 to 110.88 dB. This signifies that as the Savitzky-Golay filter is applied multiple times the better the measurement accuracy increases. However, multiple application of the Savitzky-Golay filter reduces the noise level in the signal, this becomes impractical to implement in the controller which has low computation power such as the microcontroller because it will experience computation delays owing to computational complexity. The study discovered that three times filtering is the optimum for reducing computation latency and improving signal quality.

Fig. 1: SNR for (a) maximum temperature and (b) temperature difference lithium-ion battery when Savitzky–Golay filter applied in multiple times

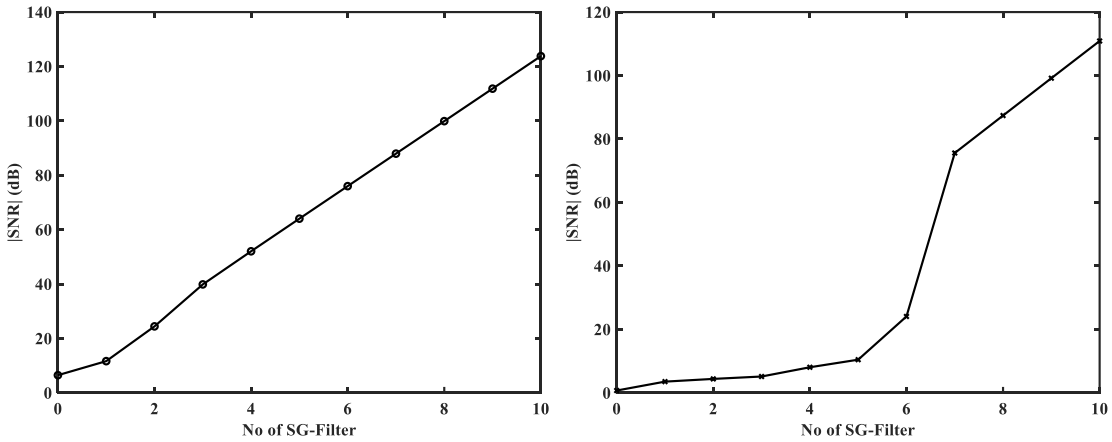

(a) (b)

CONCLUSION

In this research work, the input power from 30 W, 40 W, 50 W, and 60 W were used to reproduce the high load. The maximum surface temperature and temperature difference from the results were obtained. The maximum surface temperature and temperature difference were corrupted by the random fluctuation of the temperature which can lead to inaccurate measurement. This work uses the Savitzky-Golay filter to minimize the effect of random fluctuation noises, the results obtained after filtering were found to give great improvement in the SNR by 79.1% and 85.86% when it was applied to the maximum temperature and temperature difference, respectively. It is concluded from the results Savitzky-Golay filter is capable of boosting noisy temperature data in which the noise ratio is very low such as temperature difference which is 0.7222 in comparison to maximum temperature. Therefore, the start-up time parameter in battery thermal management can be controlled by the Savitzky-Golay filter which attenuates random temperature fluctuations of battery temperature noise and avoid the cooling system from being falsely triggered.

Article DOI: https://doi.org/10.37284/eaje.7.1.2135

Acknowledgements

The authors would like to thank the Dar es Salaam Institute of Technology (DIT) for supporting this study.

REFERENCES

[1] Hamisi, C.M., et al., *Thermal behavior of lithium-ion battery under variation of convective heat transfer coefficients, surrounding temperatures, and charging currents.* Journal of Loss Prevention in the Process Industries, 2022. **80**: p. 104922.

[2] Tran, M.-K., et al., *A review of range extenders in battery electric vehicles: Current progress and future perspectives.* World Electric Vehicle Journal, 2021. **12**(2): p. 54.

[3] Deng, Z., et al., *Sensitivity analysis and joint estimation of parameters and states for all-solid-state batteries.* IEEE Transactions on Transportation Electrification, 2021. **7**(3): p. 1314-1323.

[4] Akhoundzadeh, M.H., et al., *Investigation and simulation of electric train utilizing hydrogen fuel cell and lithium-ion battery*. Sustainable Energy Technologies and Assessments, 2021. **46**: p. 101234.

[5] Mbulu, H., Y. Laoonual, and S. Wongwises, *Experimental study on the thermal performance of a battery thermal management system using heat pipes.* Case Studies in Thermal Engineering, 2021. **26**: p. 101029.

[6] Zhang, Y., et al., *Lithium-ion battery pack state of charge and state of energy estimation algorithms using a hardware-in-the-loop validation.* IEEE Transactions on Power Electronics, 2016. **32**(6): p. 4421-4431.

[7] Zhang, W., et al., *A novel heat pipe assisted separation type battery thermal management system based on phase change material*. Applied Thermal Engineering, 2020. **165**: p. 114571.

[8] Qin, P., et al., *Experimental and numerical study on a novel hybrid battery thermal management system integrated forced-air convection and phase change material*. Energy Conversion and Management, 2019. **195**: p. 1371-1381.

[9] Liu, S., G. Zhang, and C.-Y. Wang, *Challenges and Innovations of Lithium-Ion Battery Thermal Management Under Extreme Conditions: A Review*. ASME Journal of Heat and Mass Transfer, 2023. **145**(8): p. 080801.

[10] Yang, J., Y. Cai, and C. Mi, *Lithium-ion battery capacity estimation based on battery surface temperature change under constant-current charge scenario.* Energy, 2022. **241**: p. 122879.

[11] Ma, S., et al., *Temperature effect and thermal impact in lithium-ion batteries: A review*. Progress in Natural Science: Materials International, 2018. **28**(6): p. 653-666.

[12] Katoch, S.S. and M. Eswaramoorthy. *A detailed review on electric vehicles battery thermal management system*. in *IOP conference series: materials science and engineering*. 2020. IOP Publishing.

[13] Xiong, R., L. Li, and J. Tian, *Towards a smarter battery management system: A critical review on battery state of health monitoring methods.* Journal of Power Sources, 2018. **405**: p. 18-29.

[14] Panchal, S., et al., *Cycling degradation testing and analysis of a LiFePO4 battery at actual conditions.* International Journal of Energy Research, 2017. **41**(15): p. 2565-2575.

[15] Guo, Y., et al., *Online estimation of SOH for lithium-ion battery based on SSA-Elman neural network.* Protection and Control of Modern Power Systems, 2022. **7**(3): p. 1-17.

[16] Liu, C., et al., *Strong robustness and high accuracy in predicting remaining useful life*

Article DOI: https://doi.org/10.37284/eaje.7.1.2135

of supercapacitors. APL Materials, 2022. **10** (6).

[17] Yang, S., et al., *Passive and Active Balancing*, in *Advanced Battery Management System for Electric Vehicles*. 2022, Springer. p. 165-187.

[18] Pesaran, A., S. Santhanagopalan, and G. Kim, *Addressing the impact of temperature extremes on large format li-ion batteries for vehicle applications (presentation)*. 2013, National Renewable Energy Lab.(NREL), Golden, CO (United States).

[19] Richardson, R.R., P.T. Ireland, and D.A. Howey, *Battery internal temperature estimation by combined impedance and surface temperature measurement.* Journal of Power Sources, 2014. **265**: p. 254-261.

[20] Siddique, A.R.M., S. Mahmud, and B. Van Heyst, *A comprehensive review on a passive (phase change materials) and an active (thermoelectric cooler) battery thermal management system and their limitations.* Journal of Power Sources, 2018. **401**: p. 224-237.

[21] Triwijaya, S., A. Pradipta, and T. Wati. *Automatic Design of Battery Charging System Power Supply from Photovoltaic Sources Base on Voltage*. in *Journal of Physics: Conference Series*. 2021. IOP Publishing.

[22] Jin, S., M.-S. Youn, and Y.-J. Kim. *Optimization of air-cooling system for a lithium-ion battery pack*. in *E3S Web of Conferences*. 2021. EDP Sciences.

[23] Du, J., et al., *Thermal management of air-cooling lithium-ion battery pack.* Chinese Physics Letters, 2021. **38**(11): p. 118201.

[24] Balasingam, B., *Robust Battery Management System Design With MATLAB*. 2023: Artech House.

[25] Dong, G., et al., *Online state of charge estimation and open circuit voltage hysteresis modeling of LiFePO4 battery using invariant imbedding method.* Applied Energy, 2016. **162**: p. 163-171.

[26] Li, X., C. Yuan, and Z. Wang, *Multi-time-scale framework for prognostic health condition of lithium battery using modified Gaussian process regression and nonlinear regression.* Journal of Power Sources, 2020. **467**: p. 228358.

[27] Rahimi-Eichi, H., F. Baronti, and M.-Y. Chow, *Online adaptive parameter identification and state-of-charge coestimation for lithium-polymer battery cells.* IEEE Transactions on Industrial Electronics, 2013. **61**(4): p. 2053-2061.

[28] Dong, G., et al., *Remaining dischargeable time prediction for lithium-ion batteries using unscented Kalman filter*. Journal of Power Sources, 2017. **364**: p. 316-327.

[29] Liang, J., Y. Gan, and Y. Li, Investigation on the thermal performance of a battery thermal management system using heat pipe under different ambient temperatures. Energy conversion and management, 2018. 155: p. 1-9.

[30] De Oliveira, M.A., et al., *Use of savitzky–golay filter for performances improvement of SHM systems based on neural networks and distributed PZT sensors*. Sensors, 2018. **18**(1): p. 152.

[31] Savitzky, A. and M.J. Golay, *Smoothing and differentiation of data by simplified least squares procedures.* Analytical chemistry, 1964. **36**(8): p. 1627-1639.

[32] Schmid, M., D. Rath, and U. Diebold, *Why and how Savitzky–Golay filters should be replaced.* ACS Measurement Science Au, 2022. **2**(2): p. 185-196.

[33] Liu, Y., et al., *Applications of savitzky-golay filter for seismic random noise reduction.* Acta Geophysica, 2016. **64**: p. 101-124.

[34] Chen, J., et al., *A simple method for reconstructing a high-quality NDVI time-*

Article DOI: https://doi.org/10.37284/eaje.7.1.2135

series data set based on the Savitzky–Golay filter. Remote sensing of Environment, 2004. **91**(3-4): p. 332-344.

[35] Bian, J.-h., et al., *Reconstruction of NDVI time-series datasets of MODIS based on Savitzky-Golay filter*. Journal of Remote Sensing, 2010. **14**(4): p. 725-741.

[36] Li, M. and J. Liu. *Reconstructing vegetation temperature condition index based on the Savitzky–Golay filter*. in *Computer and Computing Technologies in Agriculture IV: 4th IFIP TC 12 Conference, CCTA 2010, Nanchang, China, October 22-25, 2010, Selected Papers, Part III 4*. 2011. Springer.

[37] Ruffin, C., R.L. King, and N.H. Younan, *A combined derivative spectroscopy and Savitzky-Golay filtering method for the analysis of hyperspectral data.* GIScience & Remote Sensing, 2008. **45**(1): p. 1-15.

